Korean J. Chem. Eng., **28**(9), 1956-1963 (2011)
DOI: 10.1007/s11814-011-0056-y

Experimental and model investigation on the mass balance of a dry circulating fluidized bed for flue gas desulfurization system

Yuan Li and Changfu You†

Key Laboratory for Thermal Science and Power Engineering of Ministry of Education,
Department of Thermal Engineering, Tsinghua University, Beijing 100084, China
(*Received 20 December 2010 • accepted 4 March 2011*)

Abstract−A moderate temperature dry circulating fluidized bed flue gas desulfurization (CFB-FGD) process was developed using rapidly hydrated sorbent. This technique has the advantages of low cost, no water consumption, and a valuable dry product $CaSO_4$. To keep the system operation stable, a mass balance model, based on cell model considering flow state, particle abrasion, particle residence time, particle segregation and desulfurization processes, was built to predict the system state and optimize the operating condition. Experimental studies were conducted on a pilot-scale CFB-FGD system with rapidly hydrated sorbent made from CFB circulating ash and lime (circulating ash sorbent) or coal fly ash and lime (coal fly ash sorbent). Calculated results were compared with experimental results and the relative error was less than 10%. The results indicated that feed sorbent mass, feed sorbent size, superficial gas velocity, particle abrasion coefficient and cyclone efficiency had significant influence on the mass balance of CFB system. The circulating ash sorbent was better than the coal fly ash sorbent, for providing higher desulfurization efficiency and being better for the CFB-FGD system to achieve mass balance.

Key words: CFB-FGD, Rapidly Hydrated Sorbent, Mass Balance

INTRODUCTION

Removal of SO_2 from ue gases emitted during fossil fuel combustion has been a worldwide concern since the 1970s. Various flue gas desulfurization (FGD) technologies have been developed to remove SO_2 with Ca-based sorbents widely used because of their economic advantages, such as wet FGD [1,2], semi-dry FGD [3,4] and dry FGD [5]. A moderate temperature dry-FGD process developed for CFB was developed using rapidly hydrated sorbent [6-8]. This technique has the advantages of low cost, little water consumption, and a valuable dry product $CaSO_4$. Rapidly hydrated sorbent was prepared by hydrating coal fly ash and lime at ambient temperature for 2 hours with drying for 1.5 hours at 150 °C, providing an 83% of desulfurization efficiency at a calcium and sulfur ratio (Ca/S) of 2.0 and a bed temperature of 750 °C [7,8]. Whereas, rapidly hydrated sorbent particle abrasion caused by collisions in CFB decreased the desulfurization efficiency and Ca conversion ratio [6]. Li [9] used circulating ash from CFB boiler (circulating ash) instead of coal fly ash to prepare rapidly hydrated sorbent, which had better anti-abrasion characteristic and better desulfurization effect on a thermo-gravimetric analyzer (TGA) test.

A mass balance is the basis of stable operation for a CFB reactor, which is very important for a CFB-FGD system operating under optimum condition and obtaining high desulfurization efficiency [10,11]. Many factors, such as feed sorbent mass, superficial gas velocity and cyclone efficiency, have influence on the mass balance of CFB reactor [10,11]. For rapidly hydrated sorbent, particle abrasion is also an important factor that should be considered. Thus, it is meaningful to investigate the mass balance of dry CFB-FGD system.

Many mass balance models for CFB reactor have been proposed [11-14], with the cell model one of the most commonly used models [11,14]. In this investigation, experiments were conducted on a pilot-scale CFB-FGD experimental system, using rapidly hydrated sorbent made from circulating ash and lime (circulating ash sorbent) or coal fly ash and lime (coal fly ash sorbent). A mass balance model for the CFB reactor based on cell model was built to predict the mass balance state of the CFB-FGD system and optimize the operating condition. Flow state, particle abrasion, particle residence time, particle segregation and desulfurization process were considered in this model.

EXPERIMENT

The pilot-scale CFB reactor system is shown in Fig. 1. The main subsystems were the sorbent preparation system, the ue gas generation system and the CFB reactor. The sorbent preparation subsystem included a hydration mixer, a vacuum lter, and an infrared dryer. The ue gas generation subsystem included a fan, an oil burner, an SO_2 mixing chamber, and an air cooler. The CFB reactor included the main bed, a distributor, a cyclone separator, a bed material circulating facility, a bed material feeder and drain, a bag lter, and a compressor. Flue gas generated by the oil burner was cooled with the air cooler to produce 130 °C simulated ue gas. SO_2 was added to the ue gas before the air cooler. The CFB reactor riser was 6 m high with a 0.305 m diameter and a ue gas ow rate of 300 Nm^3/h. The ue gas passed through the CFB reactor and reacted with the sorbent, then through the cyclone separator and bag lter before being

†To whom correspondence should be addressed.
E-mail: youcf@tsinghua.edu.cn
‡This work was presented at the 8th Korea-China Workshop on Clean Energy Technology held at Daejeon, Korea, Nov. 24-27, 2010.

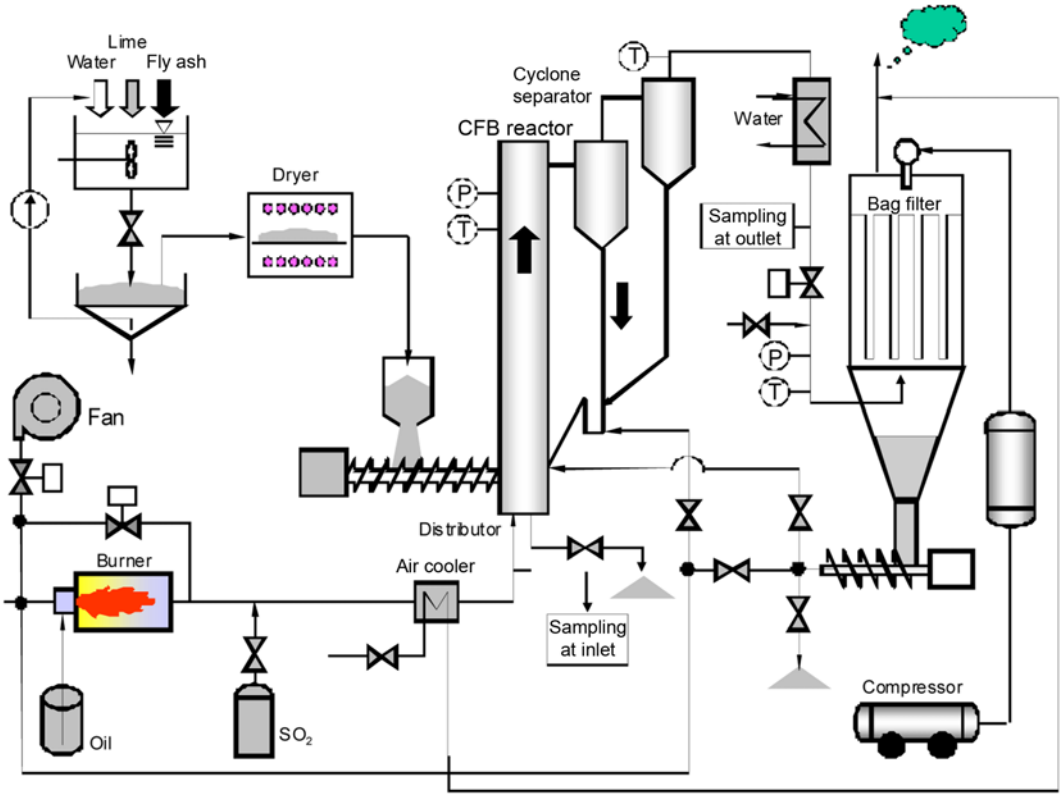

Fig. 1. Pilot-scale CFB reactor experimental system diagram.

emitted from the stack. The sorbent particles collected in the cyclone separator were fed back into the reactor for recirculation or drained out of the system [6-8].

The O_2, CO_2, and SO_2 concentrations in the ue gas were measured online at the CFB reactor inlet and outlet using infrared method with a PS3400 type flue gas analyzer (Chongqing Chuanyi analyzer CO., Ltd., SO_2 concentration ranges: 0-5,000 ppm). The desulfurization efficiency was directly calculated by the inlet and outlet SO_2 concentrations (Eq. (1)). Particle size distributions were measured by a laser diffraction instrument (Malvern Mastersizer 2000).

$$\eta_{SO_2}=\frac{C_{SO_2-in}-C_{SO_2-out}}{C_{SO_2-in}}\times 100\% \quad (1)$$

The experimental conditions were as follows: calcium and sulfur ratio, Ca/S=2.0; superficial gas velocity, U_0=2.5 m/s; bed temperature, T_{bed}=600-800 °C; bed pressure drop, ΔP=1,000 Pa; inlet SO_2 concentration, C_{SO_2-in}=1,500 ppm.

MASS BALANCE MODEL

A CFB reactor is a system including one inlet and two outlets. The whole mass balance of CFB system is shown in Fig. 2, which can be expressed by Eq. (2):

$$M_{in}=M_{out}+M_{drain} \quad (2)$$

There are three assumptions for the CFB mass balance model.

1. The particles in CFB riser move up and down; the mass flow rate of particles in radial direction can be neglected.

2. Particle abrasion and particle segregation are considered; the influence of other particle kinetic phenomena, such as particle fragmentation, particle reuniting can be neglected.

3. The bed temperature only has influence on the sulfur reaction. Its influence on CFB flow state, particle abrasion can be neglected.

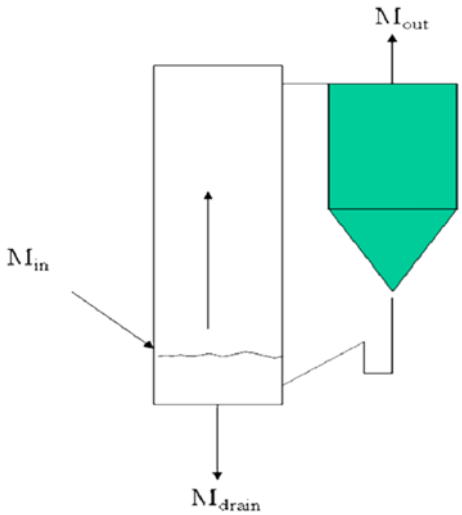

Fig. 2. Sketch of mass balance of CFB system.

1. Cell Model

To calculate details about the mass balance of CFB reactor, a cell model is introduced as the key part of the mass balance model. The CFB reactor riser (height of 6 m and diameter of 0.305 m) is divided into L cells, as shown in Fig. 3(a). In each cell, particles are divided into M parts according to their diameter (k) and N parts according

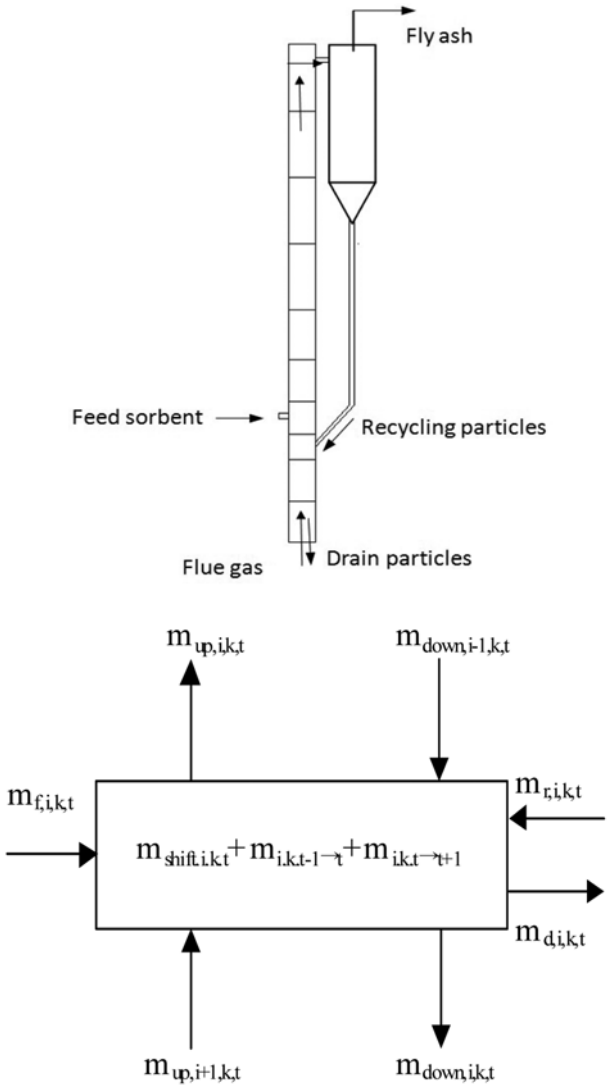

Fig. 3. Sketch of cell model: (a) Cells partition; (b) Cell mass balance.

to their residence time (t) in the CFB reactor. For each cell, there is a mass balance relationship for each part of particles shown in Fig. 3(b). The mass balance relationship can be expressed by Eq. (3).

$$\dot{m}_{f,i,k,t}+\dot{m}_{up,i+1,k,t}-\dot{m}_{up,i,k,t}+\dot{m}_{down,i-1,k,t}-\dot{m}_{down,i,k,t}+\dot{m}_{r,i,k,t}+\dot{m}_{shift,i,k,t}+\dot{m}_{i,k,t-1\to t}-\dot{m}_{i,k,t\to t+1}=0 \quad (3)$$

Where $\dot{m}_{f,i,k,t}$ is the mass flow rate of feed particles, $\dot{m}_{up,i,k,t}$ is the mass flow rate of up-particles, $\dot{m}_{down,i,k,t}$ is mass flow rate of down-particles, $\dot{m}_{r,i,k,t}$ is the mass flow rate of recycling particles, $\dot{m}_{shift,i,k,t}$ is the mass flow rate of particles caused by particle abrasion, $\dot{m}_{i,k,t-1\to t}-\dot{m}_{i,k,t\to t+1}$ is the mass flow rate of particles caused by time increasing.

2. Flow Submodel

In the cell model, mass flow rate of up-particles $\dot{m}_{up,i,k,t}$ can be calculated by Eq. (4), recommended by [15].

$$\dot{m}_{up,i,k,t}=\dot{m}_{up}(\mathrm{h})\mathrm{bed}_{i,k,t}\xi_k=\mathrm{A}(1-\varepsilon(\mathrm{h}))\rho_s(\mathrm{U}_0/\varepsilon(\mathrm{h})-\overline{\mathrm{U}}_t)\mathrm{bed}_{i,k,t}\xi_k \quad (4)$$

Void fraction at the bed height of h, ε(h), is an unknown number in Eq. (4). Thus, a flow submodel is introduced to calculate ε(h). Usually, the CFB riser includes a dense section at the lower part of the bed and a fully developed section at higher part of the bed [16]. In the dense section the void fraction is considered to be a constant, and in the fully developed section the void fraction can be expressed by Eq. (5) [17].

$$\varepsilon_k(\mathrm{h})=\varepsilon_{\infty,k}+(\varepsilon_{den,k}-\varepsilon_{\infty,k})\exp(-\alpha_k(\mathrm{h}-\mathrm{H}_{den})) \quad (5)$$

Where ε_k(h) is the void fraction at the bed height of h when all the particles are in diameter part k, $\varepsilon_{\infty,k}$ is the void fraction above the TDH when all the particles are in diameter part k, $\varepsilon_{den,k}$ is the void fraction of dense section when all the particles are in diameter part k.

In Eq. (5),can be calculated by Eqs. (6)-(10) [18],

$$\varepsilon_{\infty,k}=0.5\left[\frac{\mathrm{U}_0}{\mathrm{U}_{t,k}}+1+\frac{\mathrm{E}_{\infty,k}}{\rho_s\mathrm{U}_{t,k}}\right]-\sqrt{0.25\left[\frac{\mathrm{U}_0}{\mathrm{U}_{t,k}}+1+\frac{\mathrm{E}_{\infty,k}}{\rho_s\mathrm{U}_{t,k}}\right]^2-\frac{\mathrm{U}_0}{\mathrm{U}_{t,k}}} \quad (6)$$

$$\mathrm{E}_{\infty,k}=23.7\rho_g\mathrm{U}_0\exp\left(-5.4\frac{\mathrm{U}_{t,k}}{\mathrm{U}_0}\right) \quad (7)$$

$$\mathrm{U}_{t,k}=\sqrt{\frac{4}{3}\times\frac{\mathrm{g}\mathrm{d}_{p,k}(\rho_p-\rho_g)}{\mathrm{C}_D\rho_g}} \quad (8)$$

$$\mathrm{C}_D=\frac{24}{\mathrm{Re}_t}(1+0.15\mathrm{Re}_t^{0.687})+\frac{0.42}{1+4.25\times10^4\mathrm{Re}_t^{1.16}} \quad (9)$$

$$\mathrm{Re}_{t,k}=\frac{\mathrm{d}_{p,k}\mathrm{U}_{t,k}\rho_g}{\mu} \quad (10)$$

$\varepsilon_{den,k}$ can be calculated by following Eqs. (11)-(16) [17-19].

$$\varepsilon_{den,k}=(1-\varepsilon_{b,k})\varepsilon_{E,k}+\varepsilon_{b,k} \quad (11)$$

$$\varepsilon_{E,k}=\varepsilon_{mf,k} \quad (12)$$

$$\frac{1}{\phi_p\varepsilon_{mf,k}^3}=14 \quad (13)$$

$$\varepsilon_{b,k}=\frac{1}{1+\frac{1.3}{\mathrm{f}}(\mathrm{u}-\mathrm{u}_{mf,k})^{-0.8}} \quad (14)$$

$$\mathrm{f}=[0.26+0.7\exp(-3.3\mathrm{d}_{p,k})][0.15+(\mathrm{u}-\mathrm{u}_{mf,k})]^{-0.33} \quad (15)$$

$$\mathrm{u}_{mf,k}=\frac{\mathrm{d}_{p,k}^2(\rho_p-\rho_g)}{1650\mu}\ \ \mathrm{Re}<20 \quad (16)$$

Then, ε(h) can be calculated by Eq. (17)

$$\varepsilon(\mathrm{h})=1-\sum_1^N(1-\varepsilon_k(\mathrm{h})\mathrm{bed}_k) \quad (17)$$

3. Particle Abrasion Submodel

Particle abrasion in CFB has significant influence on the mass balance of the whole system [20-23]. A particle abrasion submodel is introduced to calculate $\dot{m}_{shift,i,k,t}$ in Eq. (3), mass flow rate of particles in part k, t caused by particle abrasion. The sketch of particle abrasion model is shown in Fig. 4. Many researches on particle abrasion in CFB have been done and some empirical formulae are proposed [21-23]. In this investigation, it is assumed that a particle in diameter part k would produce a particle in diameter park k−1 and several fine particles in diameter part 1 because of particle abrasion. Thus, $\dot{m}_{shift,i,k,t}$ can be calculated by Eq. (18).

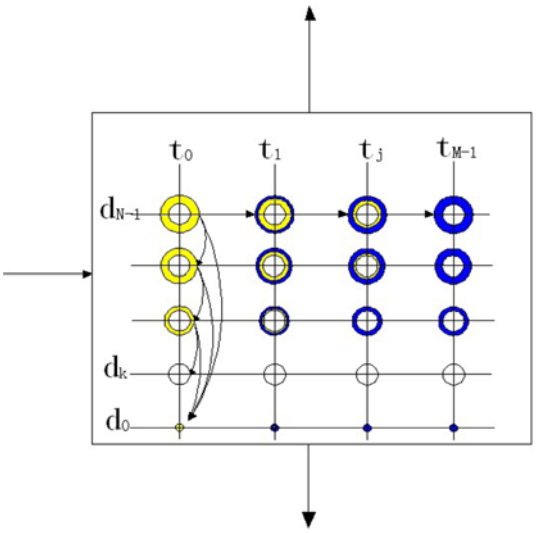

Fig. 4. Sketch of particle abrasion model and residence time model.

$$\dot{m}_{shift,i,k,t}=\begin{cases}\dot{m}_{k+1\to k,t}+\sum_{k=2}^{N}\dot{m}_{abr,k,t} & k=1\\ \dot{m}_{k+1\to k,t}-\dot{m}_{k\to k-1,t}-\dot{m}_{abr,k,t} & k=2,\ldots N-1\\ -\dot{m}_{N\to N-1,t}-\dot{m}_{abr,N,t} & k=N\end{cases} \quad (18)$$

Where $\dot{m}_{abr,k,t}$ is the mass flow rate of fine particles caused by particle abrasion from part k, t, $\dot{m}_{k\to k-1}$ is the mass flow rate of particles from part k, t to part k−1, t.

$\dot{m}_{abr,k,t}$ can be calculated by Eq. (19) [21].

$$\dot{m}_{abr,k,t}=k_a(U_0-U_{mf})m_{k,t}=k_a(U_0-U_{mf})m_{total}\times Bed_{k,t} \quad (19)$$

Where k_a is the abrasion coefficient obtained by abrasion experiments [9,24].

$$k_a=a\exp(-t/t_0)+b \quad (20)$$

$\dot{m}_{k\to k-1}$ can be calculated by Eq. (21) [14].

$$\dot{m}_{k\to k-1,t}=\frac{\bar{d}_k}{3(\bar{d}_k-\bar{d}_{k-1})}\dot{m}_{abr,k,t} \quad (21)$$

4. Particle Residence Time Submodel

Particle residence time in CFB has significant influence on the desulfurization efficiency and Ca conversion ratio [6,7]. If a particle in residence time part t stayed in CFB reactor to the next residence time part t+1, this particle would change into residence time part t+1. Particle residence time submodel (shown in Fig. 4) is introduced to calculate $\dot{m}_{i,k,t\to t+1}$.

$$\dot{m}_{i,k,t\to t+1}=\frac{m_{i,k,t}}{\Delta t} \quad (22)$$

5. Particle Segregation Submodel

In Eq. (4), ξ_k is another unknown number called segregation coefficient, which reflects particle segregation trend with different size. Particles in CFB reactor have a wide size distribution. Smaller particles have smaller terminal settling velocities and are easy to be blown up to the top of CFB reactor. Larger particles have larger terminal settling velocities and are easy to stay at the bottom of CFB reactor. Thus, particle size distributions in different cells are not the same. This phenomenon is called particle segregation. Particle segregation submodel [25,26] is introduced to calculate segregation coefficient.

$$\xi_k=1+(\xi_0-1)\cdot\left(1-\exp\left[-\frac{(\bar{U}_t-U_{t,k})}{k_1}\right]\right) \quad (23)$$

$$\xi_0=1.0+\frac{0.206}{U_0}\cdot\frac{\dot{m}_{up}(i)-G_s\cdot A}{G_s\cdot A} \quad (24)$$

$$k_1=\frac{3.0}{\bar{U}_t}\cdot U_0^2 \quad (25)$$

6. Desulfurization Submodel

To calculate desulfurization efficiency, a proper desulfurization submodel is needed. There are many desulfurization models for hydrated sorbent, such as surface coverage model [27,28], non-ideal surface adsorption model [29], shrinking core model, grain model [30] and so on. A special desulfurization model for rapidly hydrated sorbent in CFB proposed by Li [31] is used in this investigation.

$$r_{CFB}=\frac{k_s k_{diff}}{k_s+k_{diff}}\cdot\alpha\cdot\beta\cdot\varphi\cdot C_{SO_2} \quad (26)$$

$$k_a=a_1\exp\left(-\frac{E_a}{RT}\right) \quad (27)$$

$$k_{diff}=a_2\exp\left(-\frac{E_{diff}}{RT}\right)[1+a_3\exp(-a_4t)] \quad (28)$$

$$\alpha=1-a_5\exp(-a_6t) \quad (29)$$

Where k_s is the superficial reaction velocity, k_{diff} is the diffusion velocity through product layer, β is a correction factor reflected the influence of the Ca/S ratio. φ is a correction factor reflected the influence of carbon.

7. Model Solution

When all of the submodels are introduced, $bed_{i,k,t}$ and $\dot{m}_{down,i}$ are unknown numbers in the whole mass balance model. All the unknown numbers are (M*N+1)*L=M*N*L+L. Each cell has M*N mass balance equations and 1 equation for $bed_{i,k,t}$ (30).

$$\sum_{k=1}^{N}\sum_{t=1}^{M}bed_{i,k,t}=1 \quad (30)$$

Thus, there are (M*N+1)*L=M*N*L+L equations for the whole mass balance model. Then mass balance model is solved by Compaq Visual Fortran with NEQNF method from IMSL library. In this investigation, L, M, N are set to be 10.

RESULTS AND DISCUSSION

1. Experimental Results

Coal fly ash and circulating ash of CFB boiler were used as adhesive particles to make rapidly hydrated sorbent. Their components and particle size distributions were introduced by Li [9]. The experimental desulfurization efficiencies are shown in Fig. 5. To validate the model results, particle size distributions in CFB were measured and shown in Fig. 6.

As shown in Fig. 5, the desulfurization efficiency of circulating ash sorbent was 80-99% at the bed temperature of 650-750 ℃, while the desulfurization efficiency of coal fly ash sorbent was 67-83%

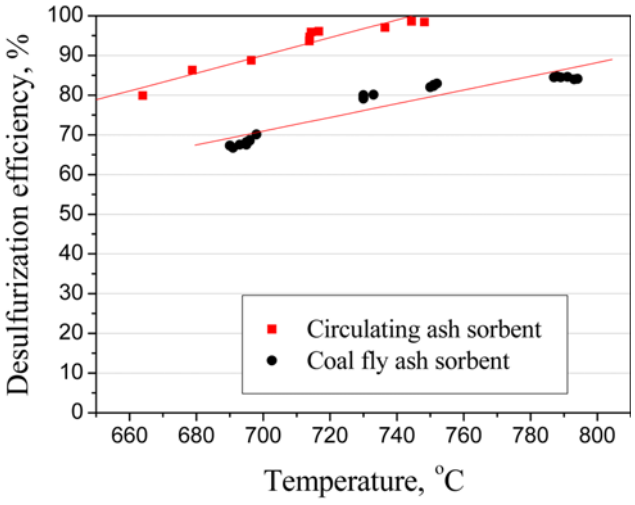

Fig. 5. Desulfurization efficiency of pilot-scale CFB-FGD system: Ca/S=2.0, U_0=2.5 m/s, T_{bed}=600-800 °C, ΔP=1,000 Pa, C_{SO_2}= 1,500 ppm.

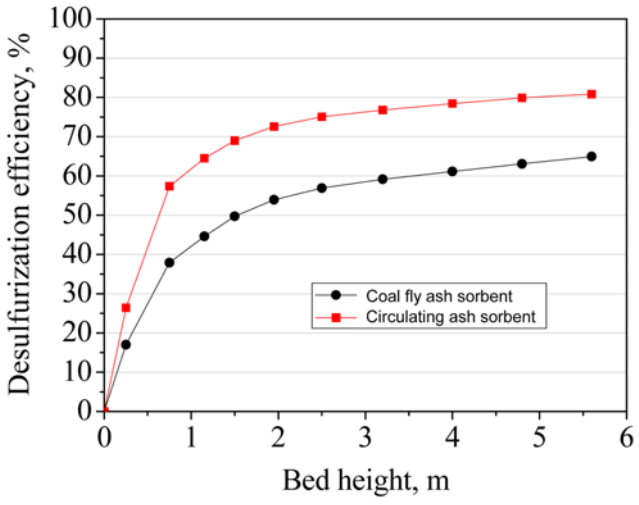

Fig. 7. Calculated desulfurization efficiency along the bed height: Ca/S=2.0, U_0=2.5 m/s, T_{bed}=700 °C, ΔP=1,000 Pa, C_{SO_2}=1,500 ppm.

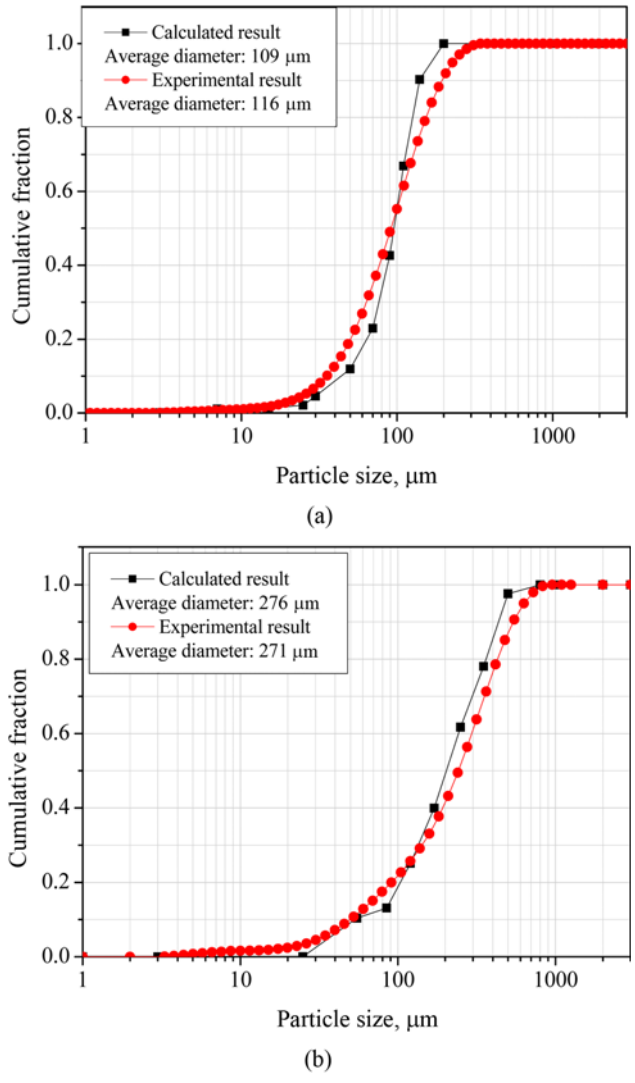

Fig. 6. Bed particle size distributions: (a) Coal fly ash sorbent; (b) Circulating ash sorbent.

at the bed temperature of 680-800 °C. Experimental results proved that using circulating ash as adhesive particle can increase the desulfurization effect of rapidly hydrated sorbent, the same with the conclusion given by Li [9].

2. Mass Balance Model Validation

To validate the mass balance model, calculated results were compared with experimental results, including bed particle size distributions and desulfurization efficiency, which are shown in Fig. 6 and Fig. 7.

Fig. 6 shows that bed particle size distributions obtained by experiment and mass balance model are similar. The relative error of average diameter is 6.0% for coal fly sorbent and 1.8% for circulating ash sorbent. Fig. 7 shows that calculated desulfurization efficiency along the bed height increases rapidly under a bed height of 2 m and then increases slowly above a bed height of 2 m. The final desulfurization efficiency of coal fly ash sorbent is 66% at the bed temperature of 700 °C and that of circulating ash sorbent is 81%. Compared with experimental results in Fig. 6, the desulfurization efficiency of coal fly ash sorbent was 70% at the bed temperature of 700 °C and that of circulating ash sorbent was 90%. The relative error is 5.7% for coal fly ash sorbent and 10% for circulating ash sorbent. Overall, the relative error of calculated results is acceptable and the mass balance model is appropriate.

3. Particle Residence Time

Particle residence time in a CFB reactor is an important parameter for rapidly hydrated sorbent particles, especially for the fine calcium-containing particles. Long residence time of fine calcium-containing particles is good for increasing desulfurization efficiency and calcium conversion ratio [6-8]. Calculated particle residence time of the two sorbent is shown in Fig. 8.

Fig. 8 shows that fine particles (smaller than 10 μm) and the largest particles (diameter part ten) in CFB reactor have shorter residence time and the residence time of other particles is almost the same; because fine particles are easy to be brought out to the bag filter, lager particles are easy to be drained and other particles recycle in CFB reactor for a longer time. Fig. 8 also shows that the residence

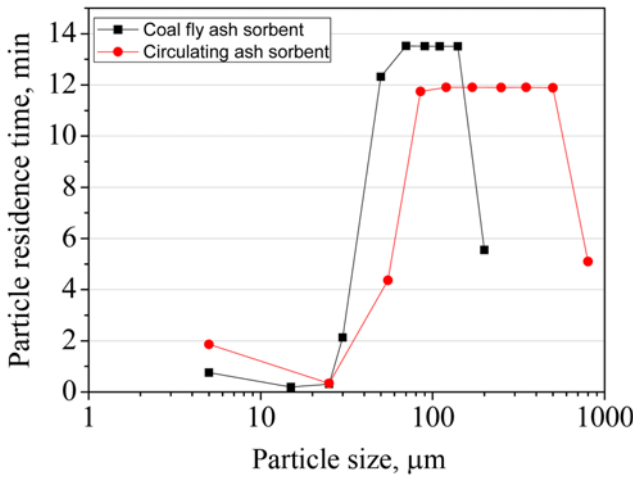

Fig. 8. Calculated particle residence time in CFB reactor.

time of fine calcium-containing particles (diameter part 1) of circulating ash sorbent is almost twice of that of the coal fly ash sorbent, proving why circulating ash sorbent has better desulfurization efficiency.

4. Particle Segregation

Fig. 9 shows the calculated average diameter of particles in each cell. It is clear that particles in lower cells are larger than those in higher cells because of particle segregation. Segregation of coal fly ash sorbent is not obvious. Its particle size range is much smaller than that of circulating ash sorbent; the terminal settling velocity difference between largest particles and fine particle is not so large like that of circulating ash sorbent, so the influence of particle segregation on coal fly ash sorbent is weaker.

5. Mass Balance Model Application

Many factors influence the mass balance of a CFB system, such as feed sorbent mass, feed sorbent size distribution, abrasion coefficient, cyclone separator efficiency and superficial gas velocity. The calculated results of cases 1-7 in Table 1 show their influence on the mass balance of CFB reactor.

Case 1 is the basic case. The fly ash ratio is 100% and no drain ash, indicating that the CFB reactor just achieves mass balance. Compared with case 7, the difference is that the feed sorbent was coal fly ash sorbent and so the feed sorbent size distribution is different. The calculated results of case 7 show that its fly ash ratio is 220% and drain ash ratio is −120%, which indicates that the CFB reactor does not achieve mass balance under this condition. This is because the coal fly ash sorbent particles are smaller than circulating ash sorbent particles; more particles are brought out to the bag filter by the cyclone separator. Thus, circulating ash sorbent is better than coal fly ash sorbent for the CFB reactor to achieve mass balance.

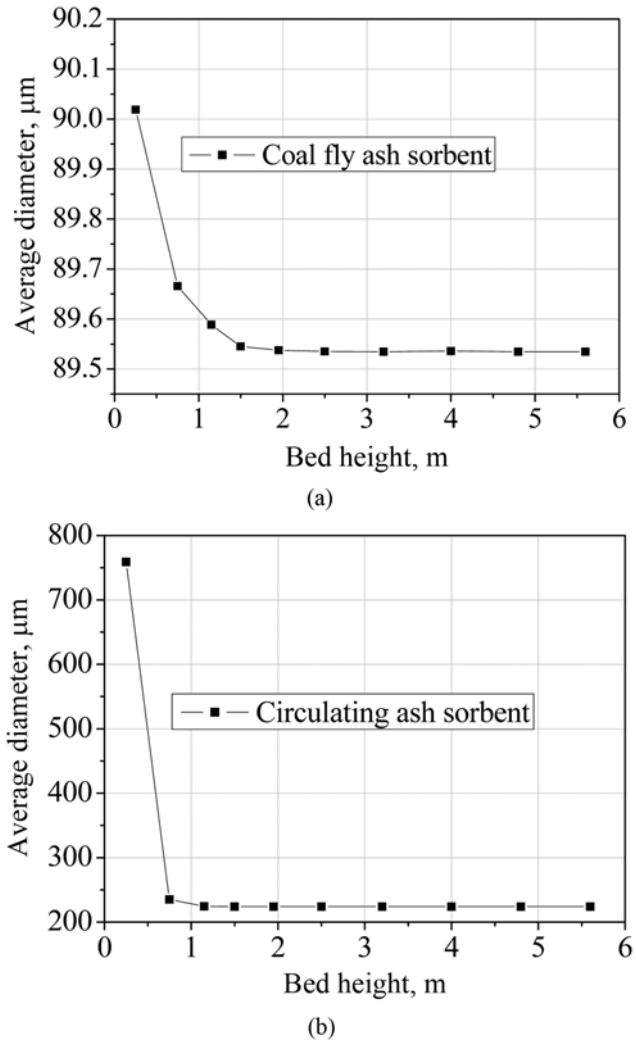

Fig. 9. Calculated particle segregation along the bed height.

Table 1. Calculated results of mass balance model

	Case No.	1	2	3	4	5	6	7
Variable	Sorbent	Circulating ash sorbent						Coal fly ash sorbent
	Feed sorbent mass	0.01	0.015	0.01	0.01	0.01	0.01	0.01
	Abrasion coefficient	a=0.00234, b=0.0001					a=0, b=0	a=0.00234, b=0.0001
	Cyclone efficiency	d_{50}=25 d_{99}=125	d_{50}=25 d_{99}=125	d_{50}=25 d_{99}=125	d_{50}=25 d_{99}=125	d_{50}=20 d_{99}=85	d_{50}=25 d_{99}=125	d_{50}=25 d_{99}=125
	Superficial gas velocity	2.5	2.5	0.5	3.5	2.5	2.5	2.5
Calculated results	Fly ash ratio, %	100	91.56	32.33	127.59	94.68	69.48	220
	Drain ash ratio, %	0	8.44	67.67	-27.59	5.32	30.52	−120
	Average diameter of bed particle, μm	301	275	249	309	285	301	109

Case 2 increases the feed sorbent mass, which increases the drain ash ratio because more large particles recycle in the CFB bed. Case 3 decreases superficial gas velocity. Compared with case 1, fly ash ratio decreases and average diameter of bed particles decreases because fewer fine particles are blown out of CFB reactor at a slower superficial gas velocity. Case 4 increases superficial gas velocity. Thus, drain ash ratio decreases to −27.59%, which indicates that the CFB system does not achieve mass balance under this condition. The CFB system should not operate under this condition, or the bed material will be blown clear. Case 5 increases cyclone separator efficiency. Compared with case 1, fly ash ratio decreases because more fine particles are recycled. Case 6 sets abrasion coefficient to be zero. Fly ash ratio decreases because no fine particles are produced because of particle abrasion in the CFB reactor.

CONCLUSIONS

Experiments were conducted on a pilot-scale CFB-FGD system using rapidly hydrated sorbent. At 650-800 °C, desulfurization efficiency increased from 67-83% to 80-99%, for circulating ash being used to prepare rapidly hydrated sorbent instead of coal fly ash.

A mass balance model of a CFB reactor was built. Compared with experimental results, the relative error of calculated results is smaller than 10%. Fine calcium-containing particles of circulating sorbent has a longer residence time in a CFB reactor, proving why circulating ash sorbent has better desulfurization efficiency.

Circulating ash sorbent is better for a CFB reactor to achieve mass balance than coal fly ash sorbent. Feed sorbent mass, feed sorbent size, superficial gas velocity, abrasion coefficient and cyclone separator efficiency have significant influence on mass balance of CFB reactor. The mass balance model of CFB reactor can be used to optimize operating condition of CFB system to achieve a better mass balance state.

ACKNOWLEDGEMENTS

This research was supported by the Special Funds for Major State Basic Research Projects (No. 2006CB200305).

NOMENCLATURE

A : cross sectional area of the CFB reactor [m^2]
$bed_{i,k,t}$: mass ratio of particles in diameter part k and residence time part t in cell i
C_D : drag force coefficient [dimensionless]
C_{SO_2-in} : inlet SO_2 concentration [ppm]
C_{SO_2-out} : outlet SO_2 concentration [ppm]
d_p : particle diameter [um]
H_{den} : height of dense section [m]
h : height above flow distributor [m]
k_a : abrasion coefficient [1/min]
k_{diff} : diffusion velocity through product layer [1/min]
k_s : superficial reaction velocity coefficient [1/min]
M_{drain} : mass flow rate of drained particles [kg/s]
M_{in} : mass flow rate of feed particles [kg/s]
M_{out} : mass flow rate of particles flew out from cyclone [kg/s]
$\dot{m}_{abr,k}$: mass flow rate of fine particles caused by abrasion from part k [kg/s]
$\dot{m}_{down,i,k,t}$: mass flow rate of down-particles [kg/s]
$\dot{m}_{f,i,k,t}$: mass flow rate of feed particles [kg/s]
$\dot{m}_{i,k,t\to t+1}$: mass flow rate of particles caused by time increasing [kg/s]
$\dot{m}_{r,i,k,t}$: mass flow rate of recycle particles [kg/s]
$\dot{m}_{shift,i,k,t}$: mass flow rate of particles caused by particle abrasion [kg/s]
$\dot{m}_{up,i,k,t}$: mass flow rate of up-particles [kg/s]
Re : Reynolds number [dimensionless]
r_{CFB} : sulfur reaction velocity [mol/min]
T_{bed} : bed temperature [°C]
U_0 : bed superficial gas velocity [m/s]
$\overline{U}_t$: average terminal settling velocity of feed particles [m/s]
$u_{mf,k}$: superficial gas velocity of Minimum fluidization state [m/s]

Greek Letters

α_k : attenuation index [1/m]
α : reaction area correction factor [dimensionless]
β : Ca/S correction factor [dimensionless]
ε_∞ : void fraction above the TDH (transport disengagement height) [dimensionless]
$\varepsilon_{b,k}$: volume fraction of bubble in dense section [dimensionless]
ε_{den} : void fraction of dense section [dimensionless]
$\varepsilon(h)$: void fraction at the bed height of h [dimensionless]
$\varepsilon_{mf,k}$: void fraction of Minimum fluidization state [dimensionless]
ϕ_p : particles sphericity [dimensionless]
φ : carbon correction factor [dimensionless]
η_{SO_2} : desulfurization efficiency of CFB-FGD system [%]
ρ_s : particle apparent density [kg/m^3]
ξ_k : segregation coefficient [dimensionless]

Subscripts

i : cell number
k : diameter part number
t : residence time part number

REFERENCES

1. H. Soud, *IEA Coal Research*, 18 (1995).
2. J. C. Sai, S. H. Wu, R. Xu, R. Sun, Y. Zhao and Y. K. Qin, *Korean J. Chem. Eng.*, **24**, 3 (2007).
3. G. W. Xu, Q. M. Guo, T. Kaneko and K. Kato, *Adv. Environ. Res.*, **4**, 9 (2000).
4. T. Zaremba, W. Mokrosz, J. Hehlmann, A. Szwalikowska and G. Stapinski, *Korean J. Chem. Eng.*, **93**, 2 (2008).
5. N. Matsushima, Y. Li, M. Nishioka, M. Sadakata, H. Y. Qi and X. C. Xu, *Environ. Sci. Technol*., **38**, 6867 (2004).
6. B. Hou, H. Y. Qi and C. F. You, *Energy Fuels*, **19**, 73 (2005).
7. J. Zhang, C. F. You, H. Y. Qi, C. H. Chen and X. C. Xu, *Environ. Sci. Technol.*, **40**, 4300 (2006).
8. J. Zhang, S. W. Zhao, C. F. You and H. Y. Qi, *Ind. Eng. Chem. Res.*, **46**, 5340 (2007).
9. Y. Li, C. F. You and C. X. Song, *Environ. Sci. Technol.*, **44**, 4692 (2010).
10. H. R. Yang, G. X. Yue, Y. Wang and J. F. Lv, *J. Eng. Thermal Energy Power*, **20**, 291 (2005).
11. H. R. Yang, X. B. Xiao, M Wirsum, G. X. Yue and F. N. Fett, *Coal*

Convers., **25**, 59 (2002).
12. Y. P. Tsuo and D. Gidaspow, *AIChE J.*, **36**, 885 (1990).
13. B. Sun and D. Gidaspow, *Ind. Eng. Chem. Res.*, **38**, 787 (1999).
14. W. D. Ni, Z. Li and X. D. Xu, *Proceedings of European Simulation Symposium*, 9 (1994).
15. Z. Y. Luo, X. T. Li, Q. H. Wang, L. M. Chen, M. J. Ni and K. F. Cen, *Power Eng.*, **14**, 19 (1994).
16. C. Y. Wen and L. H. Chen, *AIChE J.*, **28**, 117 (1982).
17. D. Kunni and O. Levenspiel, *Powder Technol.*, **61**, 193 (1990).
18. M. J. Rhodes and D. Geldart, *Powder Technol.*, **53**, 155 (1987).
19. F. Johnsson, S. Andersson and B. Leckner, *Powder Technol.*, **68**, 117 (1991).
20. U. Arena, M. D. Amore and L. Massimilla, *AIChE J.*, **29**, 40 (1983).
21. D. Merrick and J. Cullinan, *AIChE Symp. Ser.*,**70**, 366 (1974).
22. W. G. Vaux and J. S. Schruben, *AIChE Symp. Ser.*, **79**, 97 (1983).
23. L. C. Jeffrey, S. J. Khang, S. K. Lee and T. C. Keener, *Powder Technol.*, **89**, 1 (1996).
24. Y. Li, C. X. Song and C. F. You, *Energy Fuels*, **24**, 1682 (2010).
25. B. Hirschberg and J. Werther, *AIChE J.*, **44**, 25 (1998).
26. T. V. Moortel and E. Azario, *Chem. Eng. Sci.*, **53**, 1883 (1998).
27. S. M. Shih, C. S. Ho, Y. S. Song and J. P. Lin, *Ind. Eng. Chem. Res.*, **38**, 1316 (1999).
28. C. F. Liu and S. M. Shih, *Ind. Eng. Chem. Res.*, **33**, 407 (2002).
29. A. Irabien, F. Cortabitarte and M. I. Ortiz, *Chem. Eng. Sci.*, **47**, 1533 (2002).
30. J. Fernandez, A Garea and A. Irabien, *Chem. Eng. Sci.*, **25**, 1091 (1970).
31. Y. R. Li, H. Y. Qi, C. F. You and L. Z. Yang, *Korean J. Chem. Eng.*, **26**, 1155 (2009).